Compact Antenna for Picosatellites Using a Meandered Folded-Shorted Patch Array

This article has been accepted for publication in a future issue of this journal, but has not been fully edited. Content may change prior to final publication. Citation information: DOI 10.1109/LAWP.2020.2966088, IEEE Antennas and Wireless Propagation Letters

Compact Antenna for Picosatellites Using a Meandered Folded-Shorted Patch Array

Yuepei Li, Symon K. Podilchak, *Member, IEEE*, Dimitris E. Anagnostou, *Senior Member, IEEE*, Constantin Constantinides, Tom Walkinshaw

Abstract—**The design and operation of a compact antenna array offering circularly polarized (CP) radiation for picosat and other small satellites for communication applications is presented. The proposed array combines folded-shorted patches (FSPs) and meandering for antenna miniaturization. Realization of CP is achieved by a compact and planar feed circuit consisting of a network of meander-shaped 90- and 180-degree hybrid couplers which can provide quadrature feeding of the FSP elements and can be integrated onto the backside of the antenna ground plane which is only 5 cm by 5 cm. Agreement in terms of the simulations and measurements is observed with realized gain values of more than 3 dBic at 1.065 GHz and with an antenna size of $0.17\lambda_0$ by $0.17\lambda_0$.**

***Index Terms*— Folded-shorted patch (FSP) antenna, sequentially rotated arrays, circular polarisation (CP), meandering, satellite communications.**

I. Introduction

Satellites are manmade objects and are launched into space to do a specific task and can be employed for space-related research or geo-graphical surveillance [1], [2]. When compared to more conventional satellites, the development of compact satellites, such as picosats defined by a 5 cm by 5 cm by 5 cm volumetric unit, can significantly reduce launching costs and mission development time. Generally speaking, such compact satellites now provide a cost-effective approach for new scientific investigations, technology demonstrations, and advanced missions by picosatellite constellations and swarms, as well as other disaggregated systems.

When considering picosatellite-to-picosatellite, or picosatellite to more conventional satellite (and other small satellite) data communications, or, to the ground station at L-band frequencies, microstrip patch antennas are particularly attractive due to their low profile, low cost fabrication and ease of installation [3]. One option is the conventional patch antenna which has an approximate resonant length of $\lambda/2$. However, implementation on a picosatellite platform might not be possible given the size of the required 25 cm^2 antenna footprint as well as gain and mass requirements when considering PCB implementation using commercially available substrates with moderately high relative permittivity values; i.e. $\varepsilon_r \approx 10$.

In this work, compact and multilayer folded-shorted patches (FSPs) are investigated and a metallic-based demonstrator prototype is proposed for the intended picosatellite antenna application. Measurements and simulations are compared and are in agreement, considering a 2 x 2 FSP phased array which offers (CP) radiation at about 1.1 GHz. In addition, by introducing a meander for the top layer of each FSP, the size of the single-element can be reduced ($0.09\lambda_0$ by $0.08\lambda_0$ by $0.036\lambda_0$, see Figs. 1 and 2) which can miniaturize the total array while maintaining the operational frequency and achieving maximum gain values of about 4.5 dBic and total antenna efficiency of 81% for the optimized structure. To the best knowledge of the authors, no similar antenna using sequential rotation for CP and meandered elements for additional compactness, has been reported in the literature (see Table I) offering comparable gain, impedance matching bandwidth, and with reduced antenna size.

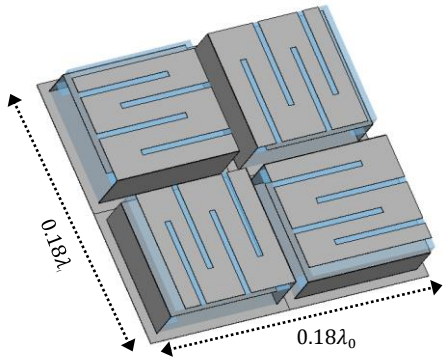

Fig. 1. Schematic of the proposed 1.1 GHz antenna for picosatellites, defined by a 2 by 2 array of sequentially rotated FSPs. The total antenna size considering an operating frequency of 1.1 GHz is 5 cm by 5 cm.

II. Design Overview for the Compact FSP Array

There are several techniques for reducing the physical size of the conventional patch antenna such as the use of high relative permittivity substrates, shorting walls, meandering, capacitive loading and slots [5]-[8]. Further size reduction can be achieved by reducing the width and length of the shorting plane while also folding of the ground plane. In [9], such a linearly polarized multiple-layer FSP antenna was reported by increasing the number of layers to adjust the resonant frequency to 2.4 GHz realizing a single-element size of $0.13\lambda_0$ by $0.14\lambda_0$ by $0.032\lambda_0$.

In [10], a dual-band structure, by interdigitated slot loading,

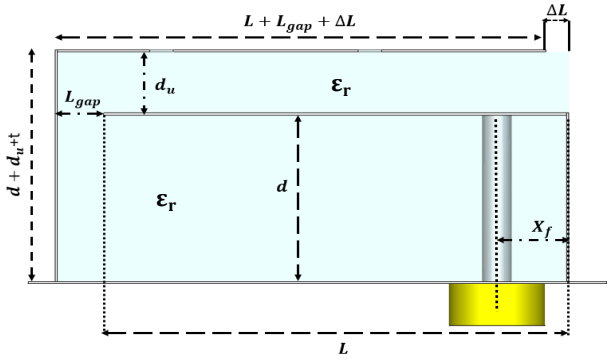

Fig. 2. Cross-section view of the single-element, two-layer FSP antenna where the dimensions are L_{gap} = 2.5 mm, d_u = 2.5 mm, L = 19 mm, W = 22 mm, t = 0.1 mm, d = 7.4 mm, ΔL = 2.8 mm, and X_f = 3.65 mm. The layers are defined at the height of $d + d_u + t$ and $d + t$, respectively. The material between the layers can be defined by εr allowing for PCB or metallic-based implementation.

This article has been accepted for publication in a future issue of this journal, but has not been fully edited. Content may change prior to final publication. Citation information: DOI 10.1109/LAWP.2020.2966088, IEEE Antennas and Wireless Propagation Letters

was reported which enabled operation at about 2.4 GHz and 5 GHz. In that work, the current on the patch surface was initially perturbed which reduced the resonant frequencies for the dual-band antenna. Then element miniaturization was made possible by the inclusion of a shorting wall and the folding of the ground plane. Another approach to reduce the size of the linearly polarized FSP was to employ a U-shaped slot within the patch as in [11]. However, reduced antenna performance was achieved due to the effective loss tangent of the PCB material. Finally, in [12] and [13], compact arrays using a 2 x 2 arrangement of sequentially rotated elements were reported for CP radiation, defined by a multilayer PCB and a fully metalized structure, respectively. Maximum gain was about 2.5 dBic for both antennas with total structure sizes of $0.2\lambda_0$ by $0.2\lambda_0$.

By following these developments, we propose a compact 5 x 5 x 1 cm^3 FSP 2x2 antenna array and supporting feeding system (see Figs. 1, 2, and 3) for CP operation at about 1 GHz. The dimensions of the single element are $0.07\lambda_0$ by $0.06\lambda_0$, while for the four-element array, the total structure size is $0.17\lambda_0$ by $0.17\lambda_0$ by $0.035\lambda_0$ considering the measured design frequency. The feeding system can be integrated on the underside of the array which can provide the needed sequentially rotated phase shifts for CP radiation. In our work, this 5-port antenna feeding system (see Fig. 3) is a defined by a network of two 90° and one 180° hybrid couplers using transmission line meandering for compactness. Also, the FSP layer lengths and widths can be determined using transmission line theory by following [13] which has accurately taken into account any open edge effects.

A. *Single-Element Design with Top Layer Meandering*

The proposed metallic-based FSP antenna element has been designed using a shorting wall with also a meandered top layer. This reduced the physical size of the top transmission line enabling compactness for the entire antenna. Also, the separation between the top and first layers was optimized for the required resonant frequency by adjusting the dimension d_u. This parameter has been varied in Fig. 4 where it is shown that the resonant frequency can be adjusted between about 1.05 GHz to 1.15 GHz given the major dimensions as outlined Table I (see Top Meandering, Metallic). Similar adjustments to the resonant frequency are possible (all results not shown for brevity) by simultaneously altering the length of the four slots on the top layer which was nominally 17.5 mm (having a 1 mm width) for operation at 1.1 GHz. Obviously, such tuning is not possible when meandering of the top layer is not considered.

The simulated current density for the single-element FSP is shown for the meandered top patch layer in the inset of Fig. 4. It can be observed that the meandering of the top layer realizes a significantly longer transmission line defining a compact

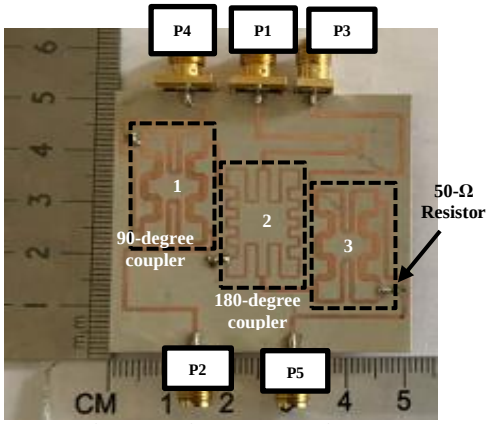

Fig. 3. Designed and fabricated feeding circuit for the array to enable CP radiation. The total dimensions of the passive circuit are 5 cm by 5 cm.

structure when compared to a more typical patch. Also, intense current densities between each parallel meandered section can be observed, which represent coupling and open edge effects.

The linearly polarized FSP antenna was also designed considering copper for all the required metal segments with a 0.1 mm thickness for the shorting wall as well as for the first and top layers. Also, 50-Ω coaxial probe feeding was employed for the individual element at an optimized position (see the caption of Fig. 2, for the relevant design dimensions) for best matching and realized gain at 1.1 GHz. Simulation results for this single element offer gain values greater than 1.5 dBi with $|S_{11}| < -15$ dB at 1.1 GHz (all results not shown for brevity).

B. *Array Design by Sequential Rotation*

A sequentially rotated array allows for the realization of CP radiation using linearly polarized elements [4]. This means that each linearly polarized antenna within the array is also fed with a sequential phase shift. For example, in the most common configuration; i.e. a 2 x 2 array, each antenna (considering a clockwise rotation) is required to have a specific phase delay of 0°, 90°, 180° and 270°. This arrangement would generate right-handed circular polarization (RHCP). To enable left-handed circular polarization (LHCP), similar 90° phase shifts would need to increase anti-clockwise [4].

Considering array theory, the larger the number of individual antenna elements used, the higher the antenna gain and the narrower the beam. In our system, we desire a compact design with increased gain, beyond the single-element, while also maintaining a broad beam and thus by using a 2 x 2 sequentially rotated array, higher gain values are expected. However, this configuration requires a feeding system (see Fig. 3) that can be bonded to the underside of the ground plane and to maintain a low-profile and compact design. Also, to achieve minimal reflection losses and optimized antenna gain in the far-field, the

TABLE I - COMPARISON TO OTHER SIMILAR FSP ANTENNAS AND ARRAYS FOUND IN THE LITERATURE CONSIDERING OPTIMIZED (SIMULATED) PARAMETERS

Work	Antenna Type	Number of layers	Single-Element or Array	Design Frequency	Reflection Coefficient	Impedance Bandwidth	Single-Element Size (Length by Width by Height)	Size of the Ground Plane	Realized Gain
[9]	Metallic	2	Single-Element	2.4 GHz	-34 dB	3%	$0.13\lambda_0$x$0.14\lambda_0$x$0.032\lambda_0$	$0.17\lambda_0$x$0.17\lambda_0$	1.6 dBi
[10]	Metallic & PCB	2	Single-Element	2.4 GHz / 5 GHz	-28 dB / -29 dB	1% / 2.5%	$0.1\lambda_0$x$0.01\lambda_0$x$0.05\lambda_0$	$0.3\lambda_0$ x$0.3\lambda_0$	3.3 dBi / 5.5 dBi
[11]	Metallic	2	Single-Element	0.84 GHz	-26 dB	19%	$0.36\lambda_0$x$0.36\lambda_0$x$0.03\lambda_0$	$0.56\lambda_0x0.56\lambda_0$	5.8 dBi
[12]	PCB	4	2x2 Array	0.4 GHz	< -10 dB	—	$0.05\lambda_0x0.04\lambda_0x0.05\lambda_0$	$0.2\lambda_0x0.2\lambda_0$	2.3 dBic
This Work Top Meandering	PCB	2	2x2 Array	0.787GHz	-17 dB	0.3%	$0.065\lambda_0$x$0.055\lambda_0$x$0.026\lambda_0$	$0.13\lambda_0$x$0.13\lambda_0$	0.606 dBic
This Work Top Meandering	PCB	2	2x2 Array	0.783GHz	-21 dB	0.45%	$0.073\lambda_0$x$0.074\lambda_0$x$0.026\lambda_0$	$0.18\lambda_0$x$0.18\lambda_0$	3.7 dBic
This Work No Meandering	Metallic	2	2x2 Array	1.1 GHz	-29 dB	0.55%	$0.08\lambda_0$x$0.08\lambda_0$x$0.036\lambda_0$	$0.18\lambda_0$x$0.18\lambda_0$	3.8 dBic
This Work Top Meandering	Metallic	2	2x2 Array	1.1 GHz	-15 dB	0.55%	$0.09\lambda_0$x$0.08\lambda_0$x$0.036\lambda_0$	$0.18\lambda_0$x$0.18\lambda_0$	4.5 dBic

This article has been accepted for publication in a future issue of this journal, but has not been fully edited. Content may change prior to final publication. Citation information: DOI 10.1109/LAWP.2020.2966088, IEEE Antennas and Wireless Propagation Letters

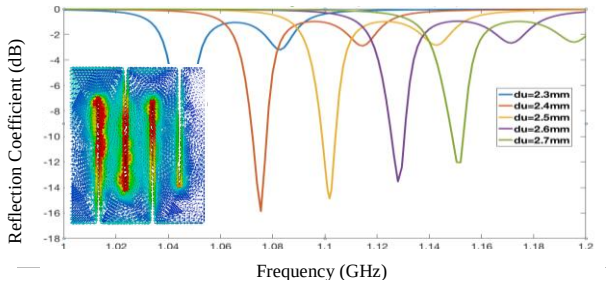

Fig. 4. Single-element $|S_{11}|$ simulation results showing the possible design frequency variation by changing the dimension d_u; i.e. the height of the top layer above the first layer (see Fig. 2) while all other parameters were maintained. In the inset, the simulated surface current density is shown for the top meandered patch. The colors for the arrows represent the current magnitude in A/m.

individual elements need to be further simulated in an array configuration considering the ground plane size (5 cm by 5 cm).

C. Feed System Design & Antenna System Operation

The fabricated and measured feeding system is shown in Fig. 3 and is a 5-port network where each port provides the required 90° phase shifts and equal power splitting. For example, port-1 can be considered the input port, with port-2 providing a 90˚ phase delay, port-3 providing a 180˚ delay, port-4 providing a 270˚ phase delay, and port-5, finally provides a 360˚ or 0˚ delay. Also, in our design we employ a high permittivity material (ε_r = 10.2 with tanδ = 0.0023) while also using meandered microstrip sections to reduce physical dimensions.

The highlighted circuit labels 1 and 3 (see Fig. 3) are the meandered 90˚ hybrid couplers where their physical dimensions have each been reduced by 70% from the standard hybrid whilst considering the same substrate. The highlighted circuit label 2, is the meandered rat-race coupler. Its physical dimensions have been reduced by 50%. Also, to conform to the dimensions of the array, the total physical dimension of the feed system was also 5 cm by 5 cm. Measured and simulation results for this optimized feeding structure suggest suitable performance; i.e. at 1.1 GHz the required phase shifts are achieved and with reflection coefficients below -20 dB (all results not shown).

The average of the transmission coefficients was -7.3 dB defining an insertion loss of around 1.3 dB which can mainly be attributed to the tanδ for the employed PCB. Moreover, the simulated realized gain for the 2x2 array is 4.5 dBic (see Table I) which does not include this feeding system loss. This defines the realized gain of the complete antenna system to be around 3.2 dBic. Given these values and a simulated efficiency of 81%, the total loss for the system (feed circuit and compact antenna) can be estimated to be about 2 dB (or a 60% total efficiency).

D. No Meandering Comparison & PCB Design Approaches

For completeness it is important to highlight the benefits of the top-layer meandering for the metallic structure with a non-meandered array whilst considering the same height and ground plane size (see Table I). This is because the electrical size of the radiating element is larger than its non-meandered counterpart. Basically, the adopted meandering allows for a more optimal 4x4 array to fit within the confines of the available physical space whilst considering the same design frequency. This enables better radiation features as outlined in Table I. For example, the realized gain is improved by about 1 dB and without a significant loss in impedance bandwidth. This is important for a compact antenna and thus ensures better CP radiation and array operation at the required design frequency.

This meandering of the top layer can also motivate further PCB implementations and fabrication simplicity. For example, if the antenna designer inserts a commercially available dielectric ($\varepsilon_r = 2.2, tan\delta = 0.0009$) forming the top-layer only (see Fig. 2), the 1.1 GHz design frequency can be adjusted to 0.787 GHz enabling further compactness. However, this will reduce the realized gain and the equivalent size of the ground plane, 0.606 dBic and $0.13\lambda_0$ by $0.13\lambda_0$, respectively (see Table I). However, antenna operation at 0.787 GHz can be improved with further optimization whilst considering a larger ground plane ($0.18\lambda_0$ by $0.18\lambda_0$) and a gain of 3.7 dBic can be achieved. In our work we consider further a compact, metallic-based antenna structure for maximum gain and to minimize any possible losses in the PCB materials.

III. Antenna Results & Assembly

By adopting the individual metallic-based FSPs and the optimized 2 x 2 array arrangement as discussed in the previous sections, reflection coefficient values are reported in Fig. 5, when simulated at the antenna inputs. It can be observed that $|S_{ii}|$ < -15 dB at 1.1 GHz for each antenna element. The realized gain maximum for the array was also 4.5 dBic (see Table I) with an 81% efficiency (defined mainly by metallic and mismatch losses) at 1.1 GHz for the optimized antenna structure without the feeding system. Also, the axial ratio was less than 3 dB over a 100° beam angle range and simulated beam pattern plots are shown in Figs. 6 and 7 at 1.065 and 1.075 GHz, respectively. See Table II for further results considering the feed circuit.

Given these simulations, the 2 x 2 sequentially rotated FSP array was fabricated and measured. All metallic sections for the FSP antenna elements were made by hand soldering and by using planar copper sheets with a 0.1 mm thickness. Also, by

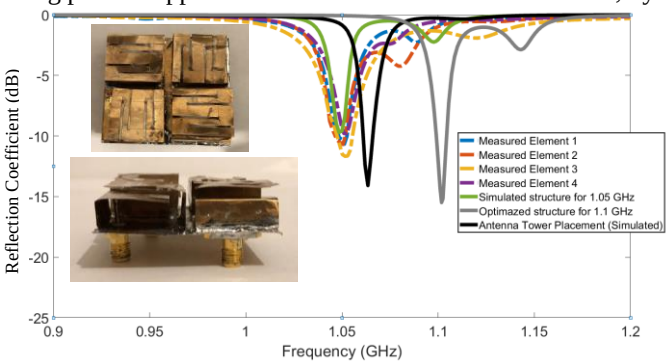

Fig. 5. Reflection coefficients at the antenna ports for the optimized and fabricated prototype in free-space. This simulation also took into account the practical fabrication tolerances. Dimensions are as follows for all elements: L_{gap} = 3 mm, d_u = 3 mm, L = 20 mm, W = 22 mm, t = 0.1 mm, d = 8 mm, ΔL = 2 m m, and X_f = 4 mm. It can be observed that the measured impedance bandwidth of 0.62% is slightly larger than the simulated (0.55%) and this discrepancy is likely related to losses introduced by the low-cost SMA connectors. Simulations are also shown when the antenna is placed on the far-field positioner (see Fig. 8, inset), where it can be observed that the S_{11} minimum was shifted to about 1.07 GHz due to the metal and plastic housing of the setup.

Table II Antenna Results Which Included the Feeding System

	Simulation (1.1 GHz)	Measurement (1.065 GHz)
RHCP gain ($\theta = 0°$)	3.2 dBic	2.9 dBic
LHCP below RHCP ($\theta = 0°$)	< 30 dB	< 20 dB
Axial Ratio < 3 dB	-80˚ < θ < +80˚	-60˚ < θ < +40˚

This article has been accepted for publication in a future issue of this journal, but has not been fully edited. Content may change prior to final publication. Citation information: DOI 10.1109/LAWP.2020.2966088, IEEE Antennas and Wireless Propagation Letters

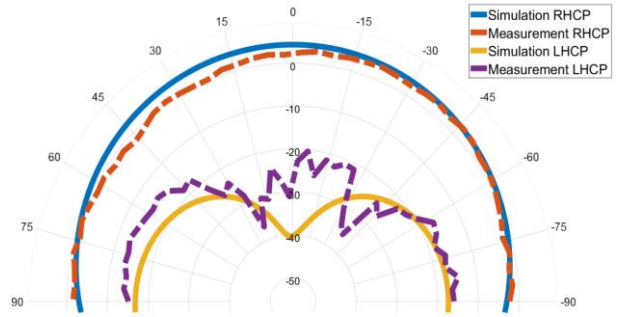

Fig. 6. Measured realized gain RHCP patterns for the CP array at 1.065 GHz. Results are shown in the x-z plane ($\phi = 0^{\circ}$) along with the cross-pol. levels.

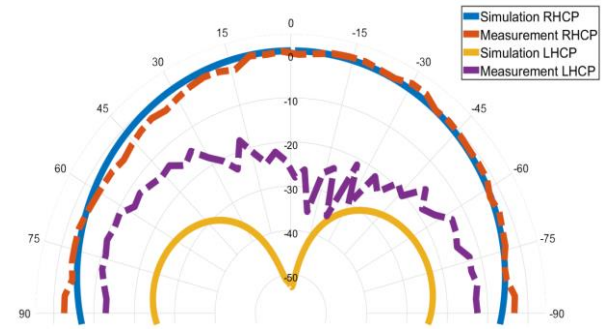

Fig. 7. Measured realized gain RHCP patterns for the CP array at 1.075 GHz. Results are shown in the x-z plane ($\phi = 0^{\circ}$) along with the cross-pol. levels.

using this copper thickness, it allowed for each shorting wall to be manually bent and soldered by hand onto the common ground plane. Similarly, for the top meandered patch layers as well as the first metallic layers, which were also soldered to the coaxial probes for 50-Ω connectivity at the antenna backside.

Since the assembly for the array was all done by hand, the patch dimensions were not perfectly consistent with the optimized simulation model. For example, at most dimensional deviations of about 0.5 mm or less were observed (see the captions of Figs. 2 and 5, and in the worst case, 1 mm) for the prototype. For example, the overall antenna height of the fabricated prototype increased from 10 mm to 11 mm, the average length of the meandered slot increased from 15 mm to 16 mm and the SMA coaxial feed probe position X_f was 4 mm, originally 3.65 mm. As expected this practicality slightly altered the resonant frequencies for the individual elements. For example, the reflection coefficient minimums are below -10 dB at 1.05 GHz as shown in Fig. 5. Once these practical values were included in the simulation model, a better agreement was observed between the simulations and the measured reflection coefficients in terms of these minimum $|S_{ii}|$ values.

The anechoic chamber at Heriot-Watt University and the PNA (Keysight N5255A) along with a far-field positioner (Dams7000) were used to measure the antenna as outlined in Table II and Figs. 6 to 8. The feeding circuit was also included. As observed, general agreement was observed with the measured beam patterns. Also, the measured maximum RHCP gain was recorded to be 2.9 dBic and 3.24 dBic at broadside (0˚) and -48˚, respectively, defining a minor beam squint. In addition, the cross-polarization levels (LHCP) are low and reach values which are 20 dB below the main beam maximum defining axial ratios which are less than 3 dB from -60° to +40°.

It should be mentioned that the far-field positioner is defined by a metal and plastic housing and this is the likely cause of the squint in the main beam pattern, the shift in resonant frequency (see Fig. 5), and the high cross-polarization levels. To

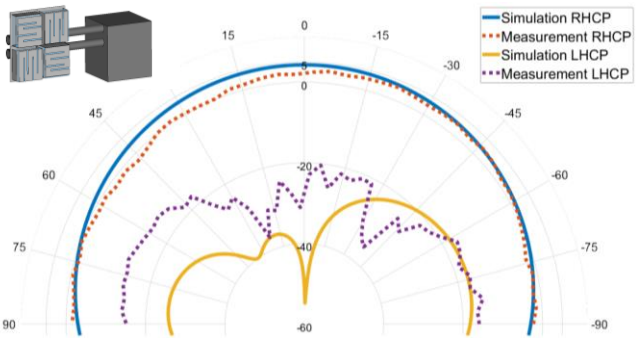

Fig. 8. Measured realized gain at 1.065 GHz for the compact FSP array, but now with the assembly tolerance and far-field positioner included in the CST simulation model (see inset).

accommodate for this, the material properties of the far-field positioner were included in CST as well as the noted assembly and fabrication dimensional tolerances. With this additional modelling, the simulated RHCP beam pattern is better matched to the measurements for the noted main beam squint (i.e. the maximum gain appeared at -20° and -30° for the simulated and measured co-pol. beam pattern, respectively) as well as the cross-polarization levels which are about 20 dB below the main beam maximum (see Fig. 8). This beam squint is also visible in the symmetry of the measured axial ratio beamwidth (see Table II). Given this practicality, that the positioner has metallic parts and is in the near-field of the antenna, results are in agreement and when considering the fabricated antenna dimensions. This defines a good proof of concept for the proposed compact array.

Preliminary results also suggest that similar antenna performance metrics can be achieved when the proposed antenna is simulated on a 5 cm by 5 cm by 5 cm picosatellite bus platform albeit a small frequency shift in the minimum of the reflection coefficients. Future design work should also include optimization of the antenna whilst considering such a satellite structure as well as the resonant tuning procedure developed in [13] using transmission line principles.

IV. Conclusions

This letter investigated a miniaturized folded-shorted patch array by using meandering for all top layers of the antenna. RHCP was achieved with measured gain in excess of 3.2 dBic. Applications for the antenna include placement on picosatellite where low data rate communications are required between other satellites enabling telemetry awareness, geo-positioning, and general connectivity at the L-band. To the authors' knowledge no similar array with such meandering, has been reported in the literature, in particular, where the antenna can offer similar gain, bandwidth, and overall compactness (see Table I).

Fabrication and measurement practicalities have also been included in the simulation model, ensuring a close agreement with the measured prototype which demonstrated a radiating bandwidth of about 2%. Future work can include additional PCB prototyping for such an antenna structure or a hybrid of metallic and dielectric materials to improve compactness whilst maintaining total antenna efficiency. For example, the top meandered metallic layer, can be realized using commercially available PCB materials with top and bottom metallic pattern etching, while the remainder of the antenna can be made using metallized folded-shorted veins as reported in this letter. The developed meandering approach can also be applied to other layers to further decrease the antenna size while also adding more layers for further structural compactness.

REFERENCES

[1] S. Gao, K. Clark, A. Sharaiha, M. Unwin, J. Zackrisson, W.A. Shiroma, J.M. Akagi, K. Maynard, P. Garner, L. Boccia, G. Amendola, G. Massa, C. Underwood, M. Brenchley, M. Pointer, and M.N. Sweeting, "Antennas for Modern Small Satellites," *IEEE Antennas and Propagation Magazine*, vol. 51, no. 4, pp. 40-56, Aug. 2009.

[2] A.H. Lokman, P.J. Soh, S. Azemi, S.K. Podilchak, S. Chalermwisutkul, M.F. Jamlos, A.A. Al-Hadi, P. Akkaraekthalin and S. Gao, "A Review of Antennas for Pico-Satellite Applications," *International Journal of Antennas and Propagation*, pp. 1 – 17, Apr. 2017.

[3] K. F. Lee and K.-F. Tong, "*Microstrip Patch Antennas*", 1st ed. London, U.K.: Imperial College Press, 2010.

[4] J. Huang, "A technique for an array to generate circular polarization with linearly polarized elements," *IEEE Transactions on Antennas and Propagation*, vol. 34, no. 9, pp. 1113–1124, Sept. 1986.

[5] K. Kan So, H. Wong, K. Man Luk , C. H. Chan, Q. Xue, "A Miniature Circularly Polarization Patch Antenna Using E-Shaped Shorting Strip", *Proceedings of the Fourth European Conference on Antennas and Propagation*, Barcelona, 2010, pp. 1-3.

[6] S. Maci, G. B. Gentili, P. Piazzesi, and C. Salvador, "Dual-band slot loaded patch antenna," in *IEE Proceedings - Microwaves, Antennas and Propagation*, vol. 142, no. 3, pp. 225–232, Jun. 1995.

[7] H.K. Kan and R.B. Waterhouse, "Size reduction technique for shorted patches," *Electron. Lett.*, vol. 35, pp. 948-949, June 1999.

[8] G. A. Mavridis, D. E. Anagnostou and M. T. Chryssomallis, "Evaluation of the Quality Factor, Q, of Electrically Small Microstrip-Patch Antennas [Wireless Corner]", *IEEE Antennas and Propagation Magazine*, Vol. 53, Is. 4, Aug. 2011, pp. 216–224.

[9] J. Zhang, and O. Berinbjerg, "Miniaturization of multiple-layer folded patch antennas". *2009 3rd European Conference on Antennas and Propagation*, pp. 2164 – 3342.

[10] D.E. Brocker, Z.H. Jiang, M.D. Gregory and D.H. Werner, "Miniaturized Dual-Band Folded Patch Antenna With Independent Band Control Utilizing an Interdigitated Slot Loading", *IEEE Transactions on Antennas Propagation*, vol. 65, no. 1, pp. 380-384, Jan. 2017.

[11] D. Kundu, A. Wasif Reza, and H. Ramiah, "Design of an U-slot Folded Shorted Patch Antenna for RF Energy Harvesting ", *2nd International Conference on Innovations in Engineering and Technology (ICCET'2014)*, Sept. 19-20, 2014 Penang (Malaysia).

[12] S.K. Podilchak, A.P. Murdoch, and Y.M.M. Antar, "Compact Microstrip-Based Folded shorted Patches", *IEEE Transactions on Antennas Propagation Magazine*, pp. 88-95, Apr., 2017.

[13] S.K.Podilchak, M. Caillet, D.Lee, Y.M.M. Antar, L.Chu, J.Cain, M. Hammar," Compact Antenna for Microsatellite Using Folded Shorted Patches and Integrated Feeding Netwrok", *IEEE Transactions on Antennas Propagation*, vol. 61, no. 9, pp. 4861-4866, Sept. 2013.